

# Numerical simulation investigation of split element modeling with variation impactor diameter effect on low-velocity impact response of unidirectional CFRP

M. Hadi Widanto<sup>1</sup>, Budi Aji Warsiyanto<sup>2</sup>, Eggy Surya<sup>3</sup>

{mhadi@unsurya.ac.id<sup>1</sup>, budiaji@unsurya.ac.id<sup>2</sup>, eggysurya@gmail.com<sup>3</sup>}

<sup>1,2</sup>Lecturer of Faculty of Aerospace Technology – Air Chief Marshal Suryadarma Aerospace University, East Jakarta 13610, Indonesia

<sup>3</sup> College Student of Aerospace Technology – Air Chief Marshal Suryadarma Aerospace University, East Jakarta 13610, Indonesia

**Abstract.** Composite material is widely used because of the advantages of strength-to-weight ratio, high stiffness, resistance to fatigue, and ease of shape in manufacturing. It is widely applied in various industries, especially the aerospace industry. In the advantages of composite materials, there are also limitations, such as the resistance of composites to out-of-plane impact loads. This load can lead to microdamage and may develop to cause catastrophic failure. This research will perform a modeling study of composite failure due to low-speed impact load. The use of split elements is performed in the model to provide a more accurate representation of the delamination failure as well as the dynamic response of the composite plate to the experimental results. This modeling is focused on determining the effect of split elements on the variable impact energy variation and impactor diameter. The results of this study indicate that split elements can improve the low velocity impact simulation model of composite plates by providing dynamic responses and delamination failures that are more in line with experimental results than without split elements. In the future, studies related to the number of split elements and the distance between split elements to the model need to be studied to determine the effect to provide better model flexibility.

**Keywords:** composites, low-velocity impact, impact response, split element

## 1. Introduction

Composite structures, used to meet the demands of lightweight materials, high strength/strength, and corrosion resistance in the aircraft industry and engineering composite fields, have become one of the materials used to repair existing structures due to their superior mechanical properties[1]. Composites are widely used for many applications in various fields such as automotive, aircraft, satellite, marine, and wind turbines due to

their advantages of high stiffness and strength with lightweight, as well as good resistance to fatigue and corrosion. CFRP (*Carbon Fiber Reinforced Polymer*) is a composite material widely used in industry because it has mechanical properties, namely high stiffness, and strength. [2]. The use of composite materials also continues to increase, especially in commercial aircraft, because of the implications for reducing exhaust emissions to the environment with a contribution of 15%-20% CO<sub>2</sub> by the 2050 target.[3].

Although this has many advantages, composite materials have disadvantages compared to metal-based materials. Composite materials have the disadvantage of being more sensitive to impact load damage than metal materials due to different damage modes [4]. Damage to impact loads can be classified into low, medium, or high velocity, depending on the parameters. Damage is divided into Barely Visible Impact Damage (BVID), minor VID (Visible Impact Damage), and large VID. Low-velocity impact (LVI) is an event that is very likely to occur in composite materials, especially on airplanes, which is caused by falling tools in the maintenance process or foreign object collisions when landing [5]. Damage due to impact loads on composite materials will decrease the residual strength and durability of the composite structure and can lead to catastrophic failure.

Based on this, studies have been conducted to evaluate composite materials' durability and failure characteristics due to impact loads, especially in the aircraft industry, which requires structural safety with high standards. In addition, the development of computer technology provides an advantage in numerical simulation because it can predict the failure picture with better time and cost efficiency. The model provide an overview to analyze a leading case on the structure. A finite element method-based Progressive Damage Model (PDM) was developed to predict the failure behavior of laminates under each load condition with a prediction approach of damage initiation followed by degradation of material stiffness. [6].

Experiments and numerical simulations of Low-Velocity Impact on composite plates on S2 glass/epoxy and aramid/epoxy fibers using LS-DYNA by combining MAT 55 with Tsai-Wu matrix damage criteria with good match results.[7]. Numerical simulation modeling of LVI using VUMAT subroutine and cohesive element with variations with full FE model (simulating the effects of interlaminar and intralaminar damage models) and reduced FE, which only simulates the effects of interlaminar delamination, which results in 50% more efficient calculation load and running time, but inconsistent peak force and stiffness values compared to the whole model [8].

This study used numerical simulation of impact loads on composite plates with variations in impact energy and impactor diameter. In predicting the impact failure of composite laminates using the hashing damage model on the intralaminar and CZM (Cohesive Zone Model) on the interlaminar. In addition, split elements are modeled on each

composite layer to determine the effect on the dynamic response and predicted failure to improve the accuracy of conformity with experimental results.

## 2. Methods

### 2.1 Intralaminar Model

The intralaminar model in this study uses Hashin's damage model, which models damage modes such as matrix tensile and matrix compression and fiber breakage tensile and fiber compression [9]. The PDM consists of three stages: linear elastic stress analysis, failure analysis, and property degrading material state variable.

$$\text{Fiber Tension } \sigma_{11} \geq 0 \quad F_f^t = \left(\frac{\sigma_{11}}{X^T}\right)^2 + \alpha \left(\frac{\tau_{12}}{S^L}\right)^2 \quad (1)$$

$$\text{Fiber Compression } \sigma_{11} < 0 \quad F_f^c = \left(\frac{\sigma_{11}}{X^c}\right)^2 \quad (2)$$

$$\text{Matrix Tension } \sigma_{22} \geq 0 \quad F_m^t = \left(\frac{\sigma_{22}}{Y^T}\right)^2 + \left(\frac{\tau_{12}}{S^L}\right)^2 \quad (3)$$

$$\text{Matrix Compression } \sigma_{22} < 0 \quad F_m^c = \left(\frac{\sigma_{22}}{2S^T}\right)^2 + \left[\left(\frac{Y^c}{2S^T}\right)^2 - 1\right] \frac{\sigma_{22}}{Y^c} + \left(\frac{\tau_{12}}{S^L}\right)^2 \quad (4)$$

Once the simulation shows that the material has reached the failure criteria where the index value has reached 1, the material properties will experience linear degradation. After that, the material will experience damage evolution to calculate the extent of the degradation of material properties. The process of the compound experiencing initiation of failure then experiencing softening stiffness (see in fig 2)

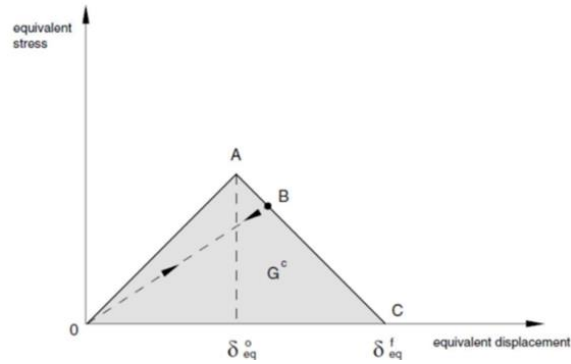


Fig. 1. Linear Damage Evolution

## 2.2 Interlaminar Model

CZM can be used to simulate interlaminar damage and its propagation. The response of the constitutive cohesive is based on two different phases: the initial damage phase and the damage evolution phase. The cohesive element method utilizes the bilinear traction-reaction law property of two separated surfaces: the relationship between  $n$  (average direction),  $s$ , and  $t$  (first and second in-plane shear) [9].

$$t = \begin{bmatrix} t_n \\ t_s \\ t_t \end{bmatrix} = \begin{bmatrix} K_{nn} & K_{ns} & K_{nt} \\ K_{ns} & K_{ss} & K_{st} \\ K_{nt} & K_{st} & K_{tt} \end{bmatrix} \begin{Bmatrix} \delta_n \\ \delta_s \\ \delta_t \end{Bmatrix} \quad (5)$$

The CZM model does not require an initial crack in the model. It then models the initiation and propagation of damage in the same analysis by defining the traction-reaction law based on the energy of strain release rate results. Modeling of failure initiation and evolution (see Fig. 2). The failure initiation model uses quadratic nominal stress criterion (QUADS) and Benzeggagh-Kenane (BK) for failure evolution.

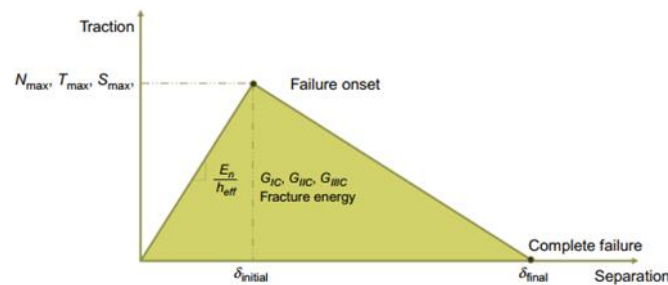


Fig. 2. kurva traction-separation law

$$\text{QUADS} \quad \left(\frac{\sigma_n}{N_{max}}\right)^2 + \left(\frac{\sigma_s}{S_{max}}\right)^2 + \left(\frac{\sigma_t}{T_{max}}\right)^2 = 1 \quad (6)$$

$$\text{Benzeggagh-Kenane (BK)} \quad G_{IC} + (G_{IIC} - G_{IC}) \left(\frac{G_{SHEAR}}{G_T}\right)^\eta = G_{TC} \quad (7)$$

### 2.3 Experiment and Numeric Model

This study aims to make modeling in analyzing the resistance of composites to impact loads with variations in energy and impactor diameter size. This research has previously been carried out experimentally. It shows that energy and impactor diameter variations can affect the impact response and damage characteristics such as dent depth.[10]. The results of this study serve as a reference for the results to be compared with the results of numerical simulations conducted by utilizing split elements. the experimental process of impact simulation on composite laminate materials is shown (see in Fig 3).

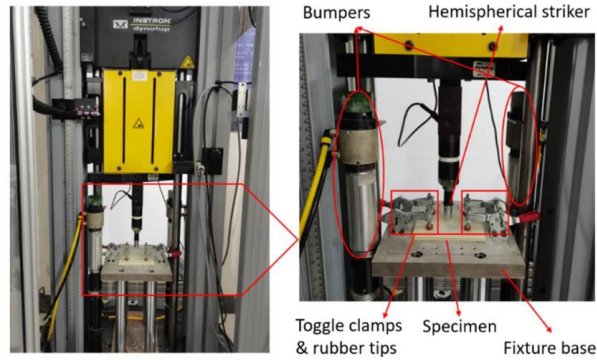


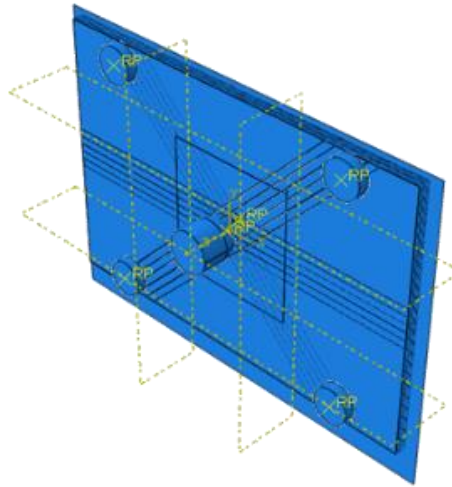
**Fig. 3.** Experiment Low Velocity Impact Laminate Composite[11]

The modeling is adjusted to the experiment where the composite plate is a T300/YH69 unidirectional carbon/epoxy plate with an autoclave with stacking layer [45/0/-45/90]4s. The prepreg results in a cured ply of 0.14 mm. Experiments were conducted concerning ASTM D7136 testing—material properties used in the numerical model (see Table 1). Impact testing was carried out with impact energy variations of 7J, 17J, and 27J with an impactor mass of 2.2 kg.

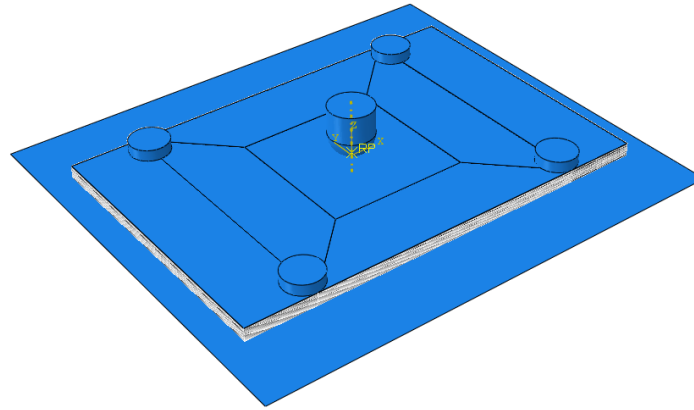
**Table 1.** Material properties T300YH/69I[10], [12]

| Property                   | Value   |
|----------------------------|---|
| Density                    | 1678 kg/m <sup>3</sup>  |
| <i>Elastic properties</i>  | $E_{11} = 140 \text{ GPa}, E_2 = E_3 = 9 \text{ Gpa}, G_{12} = G_{13} = 4.6 \text{ GPa}$<br>$G_{23} = 3.08 \text{ Gpa}, \nu_{12} = \nu_{13} = 0.32, \nu_{23} = 0.52$                    |
| <i>Strength parameter</i>  | $X^T = 1760 \text{ MPa}, X^C = 1100 \text{ MPa}, Y^T = 51 \text{ MPa},$<br>$Y^C = 130 \text{ MPa}, S^L = 70 \text{ MPa}, S^T = 60 \text{ MPa}$  |
| <i>Fracture energies</i>   | $G_{c,f}^T = 56 \text{ N/mm}, G_{c,f}^C = 10 \text{ N/mm}, G_{c,m}^T = 0.25 \text{ N/mm}$<br>$G_{c,m}^C = 0.75 \text{ N/mm}$  |
| <i>Cohesive Properties</i> | $K_{nn} = K_{ss} = K_{tt} = 180000 \text{ MPa}$<br>$\sigma_n = 60 \text{ MPa}, \sigma_s = \sigma_t = 80 \text{ Mpa.}$<br>$G_n^c = 0.35 \text{ N/mm}, G_s^c = G_t^c = 1.45 \text{ N/mm}$ |

The utilization of split elements, namely the creation of strips in the intralaminar area with a vertical shape and intersecting in the fiber direction, has been carried out and can provide quite good results. This model is then adapted to predict composite plates with variations in impactor diameter and impact energy. Will it give significant results. The split element model in this study uses six splits with a distance between splits of 3 mm (see Fig. 4a) and without split element (see Fig 4b).



(a)

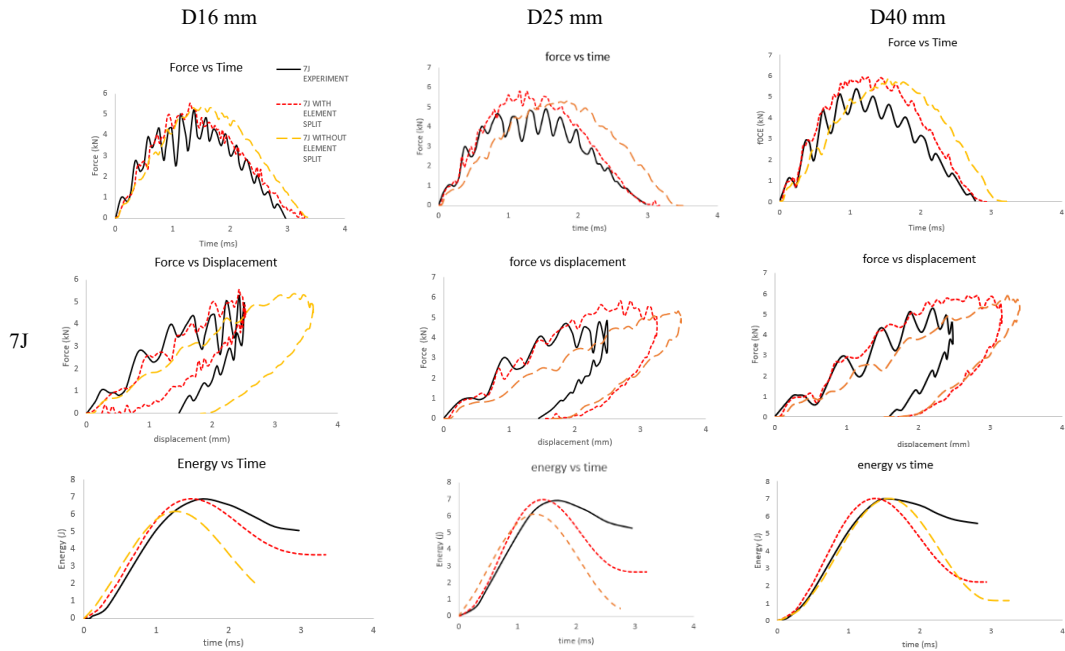


(b)

**Fig. 4.** (a) split element model in laminate composite (b) without split element

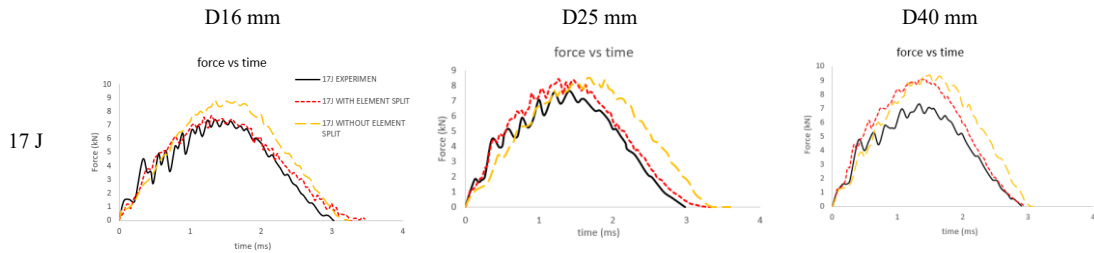
### 3 Result and Discussion

In the whole curve in figures there are black color represents the experimental results, red color represents the simulation results without split element and red color is the simulation with split element. Comparison of the dynamic response of experimental results with simulation results at an impact energy of 7 J with diameter variation (see Fig 5). The graph compares the experimental results with two models: the model using split elements and without split elements. The results show that by using split elements, the dynamic response results are better agreement with the experimental results than model without split elements. This is because the split element can describe the crack in the matrix in the lamina. In the model, the cracks in the matrix are not represented without using the split element.

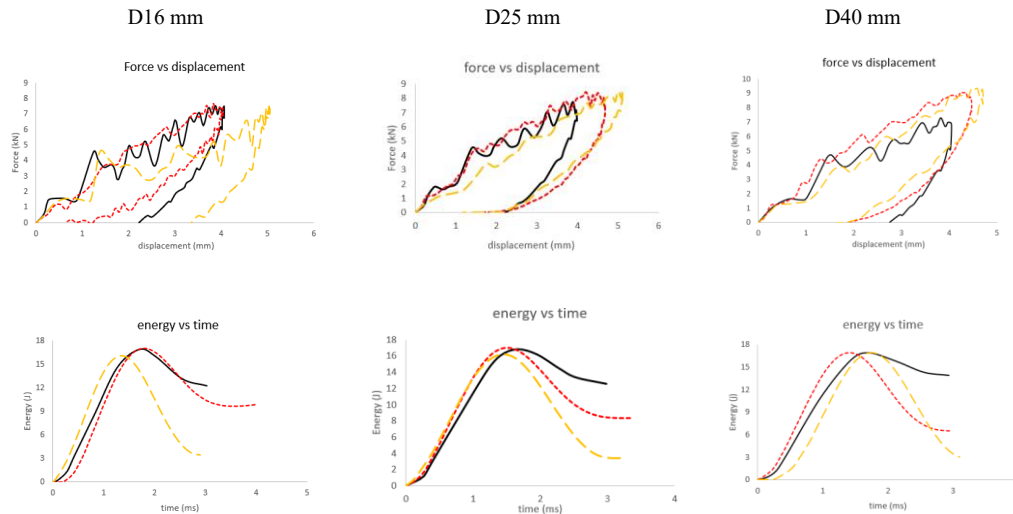


**Fig 5.** Dynamic response of composite impact energy 7J

The larger the impactor diameter causes accuracy of the dynamic response generated from the model using the split element decreases. This result can be concluded from the results of the force vs time curve at a diameter of 25 mm and 40 mm which results in a higher peak force value compared to the experimental results. The distance between split elements, which is limited to 3 mm, implies that only a small and limited area of the cracking matrix can be modeled. This effect is also seen with higher impact energy variations (see in Fig 6 & fig 7), where the more significant the diameter, the accuracy of the model with the split element decreases.



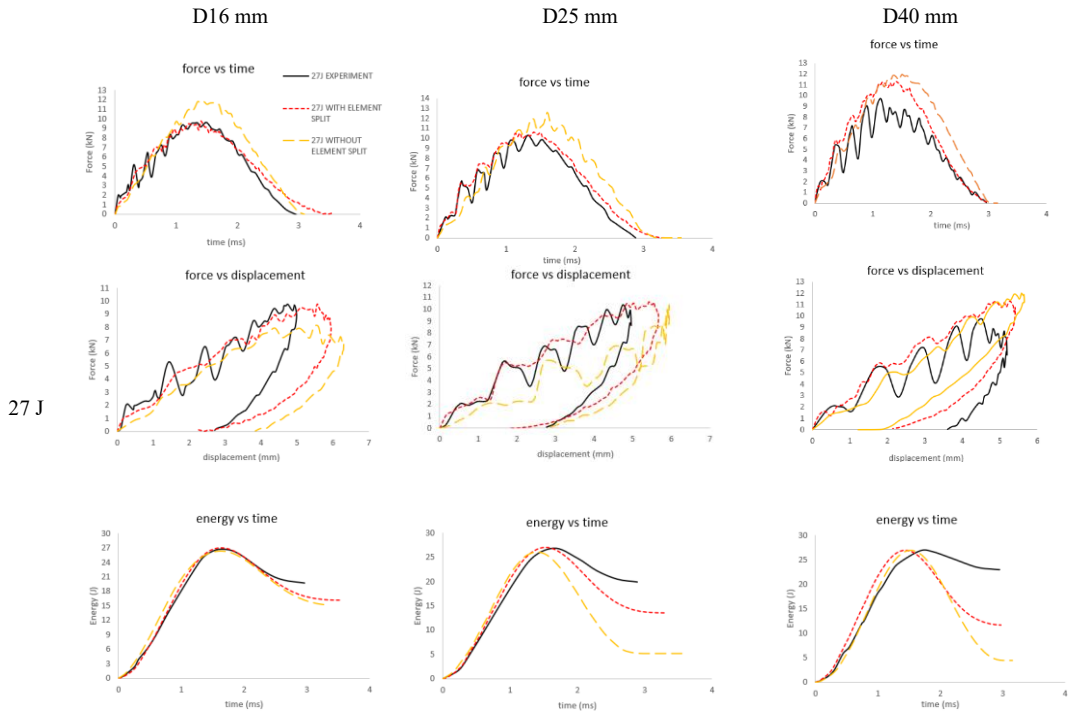




**Fig 6** Dynamic response of composite impact energy 27J

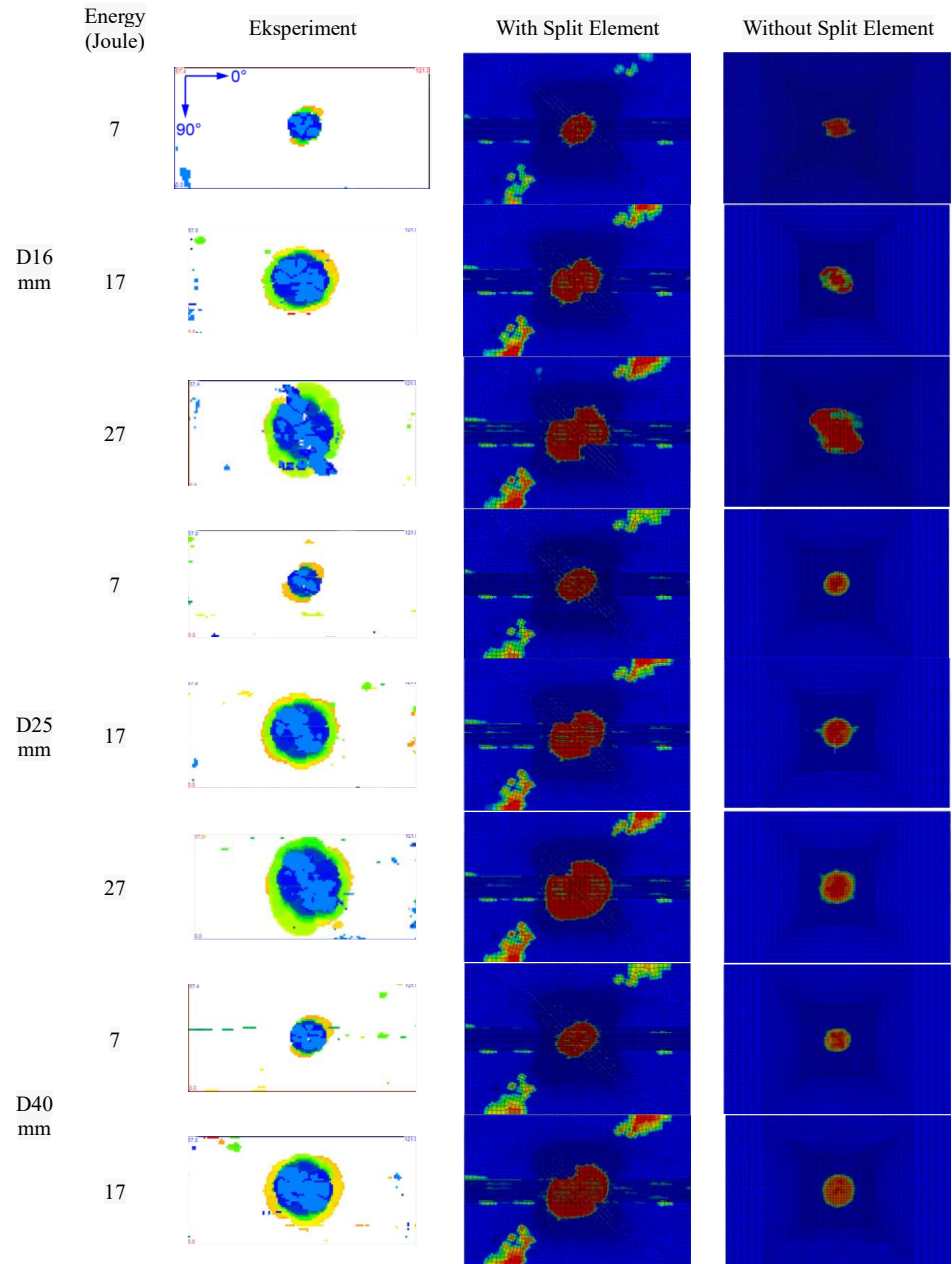
The force vs. displacement graph at each impact energy shows a graph that is quite close to the experimental results. This shows that the split element is very helpful in modeling transverse cracks and has implications for dynamic responses that reasonably correlate with experimental results. The energy vs. time graph shows a good correlation between each diameter variation and the simulated energy with the experimental results, but only up to the maximum value of energy received. Afterward, the graph shows a difference due to the different magnitude of the absorbed and unabsorbed energy values in the simulation and experimental results.

In the energy vs time curve with impact energy of 7 j (see in Fig 4) there are differences in simulation results using split element compared to experimental results. in the process of starting the impact until the maximum deflection condition the simulation results are in accordance with the experiment shown in the curve which has a good correlation, but after the maximum deflection the curve shows a difference. This difference is due to the element model used in the numerical simulation, namely the continuum shell element type where the thickness direction stress is not modeled. in addition, the intralaminar failure model using the Hashin failure's model has not included the plasticity effect of the composite material in the model. this causes the experimental and simulated energy curves to have different results.



**Fig 7.** Dynamic response of composite impact energy 27J

Overall, the simulation of low velocity impact on composite materials by utilizing split elements can provide better results than without split elements. The increase in impact energy does not have a significant effect with split elements and still provides results that are in accordance with experiments. The increasing diameter of the impactor affects the simulation results, it can be seen that the larger the impactor, the correlation of the dynamic response of simulation and experiment is increasingly incompatible. This suggests further research related to the number of split elements and the distance between split elements that can affect the dynamic response of the plate in the simulation.



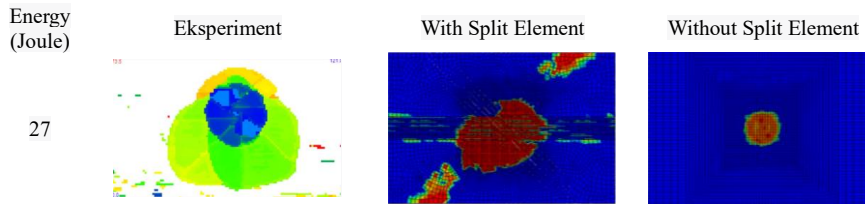


**Fig 8.** Comparison delamination area experimental and simulation result

In comparing delamination results captured in experimental and simulation results (see Fig 8). The figure shows that delamination using split elements produces more significant damage than without split elements. This is because the split element gives the effect of transverse direction cracks and can result in stress concentration in the interlaminar area. This affects the delamination failure area between the ply, which causes the area to widen. In contrast, without the split element, the vertical direction cracks are not modeled, so the delamination that occurs is only influenced by the difference in bending stiffness in each layer direction.

The delamination image in the simulation results is compared with the experiment at each energy variation and diameter variation. at an impact energy of 7 J on each diameter provides a good correlation between experimental results and simulations. At 17J and 27 J energy in the split element model the area results are quite close even though the shape is not the same. Furthermore, the use of split elements that cross diagonally from edge-to-edge causes delamination to occur in the edge area of the plate which actually does not occur in experimental results.

Comparison of parameter values to compare modeling results using and without element split (see Table 2). From these results, modeling using split elements can produce a better correlation than experimental results. The model shows that the residual displacement value cannot be appropriately captured. The model uses Hashin's damage, where the plasticity value is not included. This residual displacement deflection is primarily due to composite materials with plasticity in the shear direction.

**Table 2.** Comparison parameter result

| Diameter 16 mm        |                            |            |            |          |            |            |          |            |            |          |
|-----------------------|----------------------------|------------|------------|----------|------------|------------|----------|------------|------------|----------|
|                       | Comparison                 | 7J         |            |          | 17J        |            |          | 27J        |            |          |
|                       |                            | Experiment | Simulation | Error(%) | Experiment | Simulation | Error(%) | Experiment | Simulation | Error(%) |
| without element split | Max Impact Load (kN)       | 5.19       | 5.35       | 3.08     | 7.42       | 8.81       | 18.73    | 9.62       | 11.84      | 23.08    |
|                       | Time at the max load (ms)  | 1.36       | 1.49       | 9.56     | 1.35       | 1.34       | -0.74    | 1.48       | 1.34       | -9.46    |
|                       | Impact duration (ms)       | 2.97       | 3.34       | 12.46    | 3.02       | 3.60       | 19.21    | 2.88       | 2.95       | 2.43     |
|                       | Max displacement (mm)      | 2.5        | 3.6        | 44.00    | 4.06       | 5.04       | 24.14    | 4.99       | 6.29       | 26.05    |
|                       | Absorted Impact energy (J) | 6.79       | 6.17       | -9.13    | 16.99      | 16.09      | -5.30    | 26.74      | 26.33      | -1.53    |
|                       | Residual displacement      | 1.47       | 1.81       | 23.13    | 2.22       | 1.21       | -45.50   | 2.71       | 1.30       | -52.03   |
|                       |                            |            |            |          |            |            |          |            |            |          |
| with element split    | Comparison                 | 7J         |            |          | 17J        |            |          | 27J        |            |          |
|                       |                            | Experiment | Simulation | Error(%) | Experiment | Simulation | Error(%) | Experiment | Simulation | Error(%) |
|                       | Max Impact Load (kN)       | 5.19       | 5.43       | 4.62     | 7.42       | 7.56       | 1.89     | 9.62       | 9.75       | 1.35     |
|                       | Time at the max load (ms)  | 1.36       | 1.29       | -5.15    | 1.35       | 1.20       | -11.11   | 1.48       | 1.39       | -6.08    |
|                       | Impact duration (ms)       | 2.97       | 3.29       | 10.77    | 3.02       | 3.46       | 14.57    | 2.88       | 3.29       | 14.24    |
|                       | Max displacement (mm)      | 2.5        | 2.53       | 1.20     | 4.06       | 4.02       | -0.99    | 4.99       | 5.94       | 19.04    |
|                       | Absorted Impact energy (J) | 6.79       | 6.89       | 1.47     | 16.99      | 19.99      | 17.66    | 26.74      | 26.99      | 0.93     |
| Residual displacement | 1.47                       | 0.24       | -83.67     | 2.22     | 0.67       | -69.82     | 2.71     | 0.01       | -99.63     |          |
| Diameter 25 mm        |                            |            |            |          |            |            |          |            |            |          |
| without element split | Comparison                 | 7J         |            |          | 17J        |            |          | 27J        |            |          |
|                       |                            | Experiment | Simulation | Error(%) | Experiment | Simulation | Error(%) | Experiment | Simulation | Error(%) |
|                       | Max Impact Load (kN)       | 4.49       | 5.32       | 18.49    | 7.10       | 8.47       | 19.30    | 10.28      | 12.59      | 22.47    |
|                       | Time at the max load (ms)  | 1.05       | 1.85       | 76.19    | 1.57       | 1.69       | 7.64     | 1.30       | 1.60       | 23.08    |
|                       | Impact duration (ms)       | 2.97       | 3.5        | 17.85    | 2.98       | 3.64       | 22.15    | 2.88       | 3.55       | 23.26    |
|                       | Max displacement (mm)      | 2.48       | 3.62       | 45.97    | 3.99       | 5.11       | 28.07    | 4.93       | 5.95       | 20.69    |
|                       | Absorted Impact energy (J) | 6.93       | 6.12       | -11.69   | 16.84      | 16.15      | -4.10    | 26.81      | 26.06      | -2.80    |
| Residual displacement | 1.44                       | 0.79       | -45.14     | 2.22     | 0.83       | -62.61     | 2.76     | 0.92       | -66.67     |          |
| with element split    | Comparison                 | 7J         |            |          | 17J        |            |          | 27J        |            |          |
|                       |                            | Experiment | Simulation | Error(%) | Experiment | Simulation | Error(%) | Experiment | Simulation | Error(%) |
|                       | Max Impact Load (kN)       | 4.49       | 5.82       | 29.62    | 7.10       | 8.42       | 18.59    | 10.28      | 10.63      | 3.40     |
|                       | Time at the max load (ms)  | 1.05       | 1.16       | 10.48    | 1.57       | 1.26       | -19.75   | 1.30       | 1.39       | 6.92     |
|                       | Impact duration (ms)       | 2.97       | 3.19       | 7.41     | 2.98       | 3.33       | 11.74    | 2.88       | 3.29       | 14.24    |
|                       | Max displacement (mm)      | 2.48       | 3.25       | 31.05    | 3.99       | 4.67       | 17.04    | 4.93       | 5.66       | 14.81    |
|                       | Absorted Impact energy (J) | 6.93       | 6.99       | 0.87     | 16.84      | 16.99      | 0.89     | 26.81      | 26.99      | 0.67     |
| Residual displacement | 1.44                       | 0.05       | -96.53     | 2.22     | 0.05       | -97.75     | 2.76     | 0.06       | -97.83     |          |
| Diameter 40 mm        |                            |            |            |          |            |            |          |            |            |          |
| without element split | Comparison                 | 7J         |            |          | 17J        |            |          | 27J        |            |          |
|                       |                            | Experiment | Simulation | Error(%) | Experiment | Simulation | Error(%) | Experiment | Simulation | Error(%) |
|                       | Max Impact Load (kN)       | 5.38       | 5.88       | 9.29     | 7.29       | 9.37       | 28.53    | 9.73       | 11.97      | 23.02    |
|                       | Time at the max load (ms)  | 1.08       | 1.55       | 43.52    | 1.33       | 1.39       | 4.51     | 1.14       | 1.49       | 30.70    |
|                       | Impact duration (ms)       | 2.77       | 3.25       | 17.33    | 2.90       | 3.09       | 6.55     | 2.96       | 3.14       | 6.08     |
|                       | Max displacement (mm)      | 2.47       | 3.4        | 37.65    | 4.04       | 4.70       | 16.34    | 5.18       | 5.64       | 8.88     |
|                       | Absorted Impact energy (J) | 6.94       | 6.99       | 0.72     | 16.98      | 16.99      | 0.06     | 26.84      | 26.99      | 0.56     |
| Residual displacement | 1.59                       | 0.02       | -98.74     | 2.76     | 0.05       | -98.19     | 3.60     | 0.09       | -97.50     |          |
| with element split    | Comparison                 | 7J         |            |          | 17J        |            |          | 27J        |            |          |
|                       |                            | Experiment | Simulation | Error(%) | Experiment | Simulation | Error(%) | Experiment | Simulation | Error(%) |
|                       | Max Impact Load (kN)       | 5.38       | 5.9        | 9.67     | 7.29       | 9.05       | 24.14    | 9.73       | 11.27      | 15.83    |
|                       | Time at the max load (ms)  | 1.08       | 1.16       | 7.41     | 1.33       | 1.43       | 7.52     | 1.14       | 1.16       | 1.75     |
|                       | Impact duration (ms)       | 2.77       | 2.93       | 5.78     | 2.90       | 2.96       | 2.07     | 2.96       | 2.96       | 0.00     |
|                       | Max displacement (mm)      | 2.47       | 3.15       | 27.53    | 4.04       | 4.47       | 10.64    | 5.18       | 5.41       | 4.44     |
|                       | Absorted Impact energy (J) | 6.94       | 6.99       | 0.72     | 16.98      | 16.99      | 0.06     | 26.84      | 26.99      | 0.56     |
| Residual displacement | 1.59                       | 0.03       | -98.11     | 2.76     | 0.04       | -98.55     | 3.60     | 0.02       | -99.44     |          |

## 4 Conclusions

This research has conducted an analysis related to the development of numerical models in Low Velocity Impact on composite materials. The use of split elements in numerical simulations aims to portray the cracking matrix in the lamina that it influences the dynamic response and delamination. The variation of diameter impactor and energy variation have been carried out and the use of split elements provides a better correlation between simulation and experiment. Although it provides a good agreement, it is necessary to further examine the effect of the distance between the split element and the quantity. The larger the impactor diameter and impact energy gives a dynamic response and delamination that is increasingly different from the experimental results. Therefore, further research needs to be given to provide a more effective model for predicting the dynamic response and damage to composites in meso models.

## References

- [1] A. McIlhagger, E. Archer, and R. McIlhagger, “Manufacturing processes for composite materials and components for aerospace applications,” in *Polymer Composites in the Aerospace Industry*, Elsevier, 2019, pp. 59–81. doi: 10.1016/B978-0-08-102679-3.00003-4.
- [2] W. Zhuang, P. Wang, W. Ao, and G. Chen, “Experiment and Simulation of Impact Response of Woven CFRP Laminates with Different Stacking Angles,” *J Shanghai Jiaotong Univ Sci*, vol. 26, no. 2, pp. 218–230, Apr. 2021, doi: 10.1007/s12204-021-2271-y.
- [3] J. Bachmann, C. Hidalgo, and S. Bricout, “Environmental analysis of innovative sustainable composites with potential use in aviation sector—A life cycle assessment review,” *Sci China Technol Sci*, vol. 60, no. 9, pp. 1301–1317, 2017, doi: 10.1007/s11431-016-9094-y.
- [4] A. S. Al Omari, K. S. Al-Athel, A. F. M. Arif, and F. A. Al-Sulaiman, “Experimental and computational analysis of low-velocity impact on carbon-, glass- and mixed-fiber composite plates,” *Journal of Composites Science*, vol. 4, no. 4, 2020, doi: 10.3390/jcs4040148.
- [5] X. C. Sun and S. R. Hallett, “Barely visible impact damage in scaled composite laminates: Experiments and numerical simulations,” *Int J Impact Eng*, vol. 109, pp. 178–195, 2017, doi: 10.1016/j.ijimpeng.2017.06.008.
- [6] J. Zhou, P. Wen, and S. Wang, “Finite element analysis of a modified progressive damage model for composite laminates under low-velocity impact,” *Compos Struct*, vol. 225, Oct. 2019, doi: 10.1016/j.compstruct.2019.111113.
- [7] B. Berk *et al.*, “An experimental and numerical investigation on low velocity impact behavior of composite plates,” *J Compos Mater*, vol. 50, no. 25, 2016, doi: 10.1177/0021998315622805.

- [8] D. Feng and F. Aymerich, "Finite element modelling of damage induced by low-velocity impact on composite laminates," *Compos Struct*, vol. 108, no. 1, 2014, doi: 10.1016/j.compstruct.2013.09.004.
- [9] P. P. Camanho, C. G. Dávila, and M. F. De Moura, "Numerical simulation of mixed-mode progressive delamination in composite materials," *J Compos Mater*, vol. 37, no. 16, 2003, doi: 10.1177/0021998303034505.
- [10] H. Cao *et al.*, "Experimental investigation of impactor diameter effect on low-velocity impact response of CFRP laminates in a drop-weight impact event," *Materials*, vol. 13, no. 18, Sep. 2020, doi: 10.3390/ma13184131.
- [11] M. Bin Rahman and L. Zhu, "Low-Velocity Impact Response on Glass Fiber Reinforced 3D Integrated Woven Spacer Sandwich Composites," *Materials*, vol. 15, no. 6, Mar. 2022, doi: 10.3390/ma15062311.
- [12] B. Liao *et al.*, "An explicit–implicit combined model for predicting residual strength of composite cylinders subjected to low velocity impact," *Compos Struct*, vol. 247, Sep. 2020, doi: 10.1016/j.compstruct.2020.112450.